

New Detectors for the Kaon and Hypernuclear Experiments with KaoS at MAMI and with PANDA at GSI

P. Achenbach,* C. Ayerbe Gayoso, R. Böhm, M.O. Distler, J. Friedrich, K.W. Krygier, H. Merkel, U. Müller, R. Neuhausen, L. Nungesser, J. Pochodzalla, A. Sanchez Lorente, S. Sánchez Majos, and Th. Walcher

Institut für Kernphysik, Johannes Gutenberg-Universität Mainz, Germany

J. Gerl, M. Kavatsyuk, I. Kojouharov, N. Saito, T.R. Saito, and H. Schaffner
GSI, Darmstadt, Germany

T. Bressani, S. Bufalino, and A. Feliciello

Dipartimento di Fisica Sperimentale, Università di Torino and INFN Sezione di Torino, Italy

A. Pantaleo and M. Palomba

Dipartimento di Fisica, Università di Bari, and INFN Sezione di Bari, Italy

G. Raciti and C. Sfienti

Dipartimento di Fisica, Università di Catania, and INFN Sezione di Catania, Italy

M. Agnello, F. Ferro, F. Iazzi, and K. Szymanska

Dipartimento di Fisica del Politecnico di Torino, Italy

P.-E. Tegnér

Department of Physics, Stockholm University, Sweden

B. Cederwall

Department of Physics, Royal Institute of Technology, Stockholm, Sweden

L. Majling

*Nuclear Physics Institute, Academy of Sciences of the Czech Republic, Rez near Prague, Czech Republic
(A1 Collaboration and HyperGamma Collaboration)*

The KaoS spectrometer at the Mainz Microtron MAMI, Germany, is perceived as the ideal candidate for a dedicated spectrometer in kaon and hypernuclei electroproduction. KaoS will be equipped with new read-out electronics, a completely new focal plane detector package consisting of scintillating fibres, and a new trigger system. First prototypes of the fibre detectors and the associated new front-end electronics are shown in this contribution. The Mainz hypernuclei research program will complement the hypernuclear experiments at the planned FAIR facility at GSI, Germany. At the proposed antiproton storage ring the spectroscopy of double Λ hypernuclei is one of the four main topics which will be addressed by the PANDA Collaboration. The experiments require the operation of high purity germanium (HPGe) detectors in high magnetic fields ($B \approx 1$ T) in the presence of a large hadronic background. The performance of high resolution Ge detectors in such an environment has been investigated.

1. Strange Hadrons with KaoS at MAMI

Strangeness production in the energy regime 1 – 2 GeV is undergoing a renewed interest, both theoretically and experimentally. On the theoretical side, due to the non-perturbative nature of Quantum Chromodynamics (QCD) at low energies, kaon electroproduction cannot be described by the fundamental equations for the dynamics of (asymptotically free) quarks and gluons. Instead, isobaric models are commonly used, where the hadrons are treated as effective degrees of freedom. The partonic constituents can also be considered along the lines of chiral models, which take an important feature of low energy QCD into account, namely the chiral symmetry and its spontaneous breakdown. Although lattice QCD calculations are not yet relevant to kaon production, it is anticipated that precise experimental data on

strangeness production will challenge and improve our understanding of the strong interaction in the low energy regime of QCD.

Experimentally, the conservation of strangeness in electromagnetic and strong interactions allows the tagging of baryonic systems with open strangeness, e.g. baryon resonances or hypernuclei, by detecting a kaon in the final channel. Currently, only few high quality data points exist on $K^+\Lambda$ electroproduction close to threshold, the available information on $K^+\Sigma^0$ is even more sparse. This field of physics will be addressed at Mainz Microtron MAMI, Germany, with the KaoS spectrometer.

KaoS is a very compact magnetic spectrometer suitable especially for the detection of kaons. It was built for the GSI in Darmstadt, Germany, for heavy ion induced experiments [1]. During May and June 2003 the KaoS magnets together with associated electronics and detectors were brought to Mainz. As a pilot experiment on kaon electroproduction, the separation of transverse and longitudinal structure functions in parallel kinematics is planned [2]. For the pilot exper-

*E-mail address: patrick@kph.uni-mainz.de

iment only the detection of positive kaons at moderate angles, $\theta \sim 10^\circ$, is required. With the available detector package charged particle trajectories can be measured by using two multi-wire chambers of 120 cm length. Furthermore, time-of-flight (TOF) and trigger information can be obtained from a segmented scintillator array. The use of KaoS as a two arm spectrometer for the electroproduction of hypernuclei at MAMI requires the detection of the scattered electron at laboratory angles close to 0° with typical momenta of 650 MeV/c. The kaon detector in the focal plane has to cover a range of scattering angles around 5° in coincidence. In order to cope with the special kinematics for electroproduction of hypernuclei and with the high rates background rates, KaoS will be equipped with new read-out electronics, a completely new focal plane detector package for the electron arm, and a new trigger system.

1.1. Development of new Focal Plane Detectors

The main focal plane detector of the KaoS electron arm will consist of 2 horizontal planes of fibre arrays, covering an active area of $1500 \times 500 \text{ mm}^2$, and comprising close to 2000 channels per plane (63 detectors on 21 triple boards). Each plane is divided into 58.4 mm wide triple detectors which consist of 384 fibres in three joined fibre segments coupled to three multi-anode photomultipliers (MAPMTs) and Cockcroft-Walton voltage multipliers mounted on a single 96-channel front-end board. A prototype triple detector was built and tested, see Fig. 1 for a photograph.

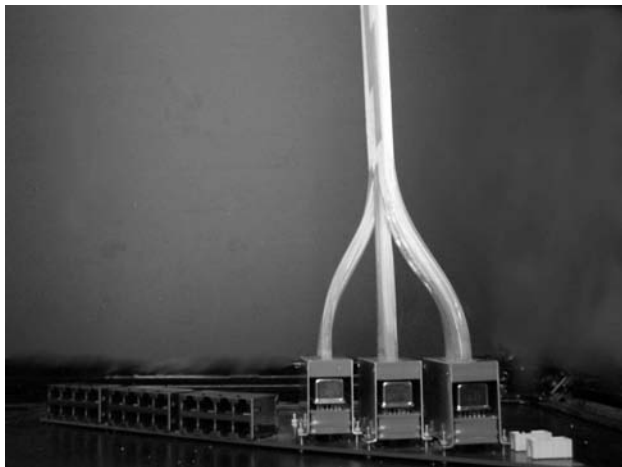


Figure 1: Photograph of a prototype triple detector with three joined fibre bundles of 58.4 mm width, bare MAPMTs, and Cockcroft-Walton voltage multipliers mounted on a single front-end board.

A fibre doublet structure is formed from two single layers of fibres, with one of the fibre layers off-set rela-

tive to the other by half a fibre spacing. The virtue of this configuration is the high fraction of overlapping fibres, i.e. a high detection efficiency, and a small pitch leading to a good spatial resolution. Several of such double layers are introduced if the number of photoelectrons per fibre is too small to be detected with the required efficiency.

The fibres are of type Kuraray SCSF-78 with double cladding and of 0.83 mm outer diameter. The cladding thickness is 0.1 mm, leading to a 0.73 mm core of refractive index $n_{core} = 1.6$. Four fibres are grouped to one channel and brought to one pixel of the MAPMT.

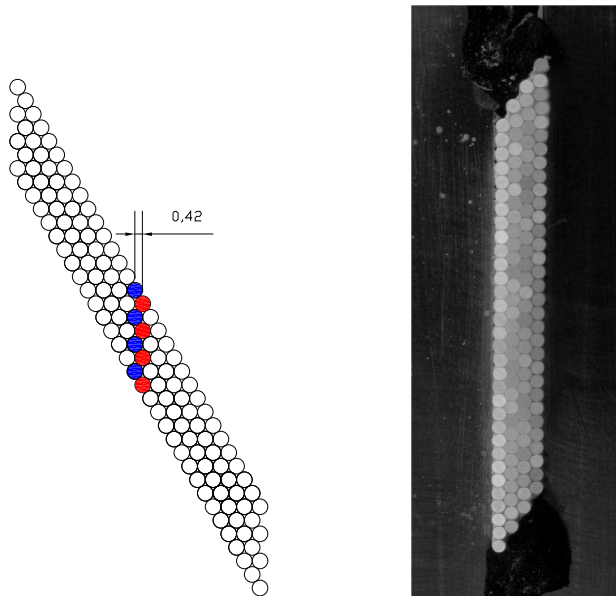


Figure 2: Scheme of a 60° column angle configuration with 4 double layers and a pitch of 0.42 mm (left) and a photograph of an assembled 60° fibre bundle (right).

The MAPMTs of type R7259K from Hamamatsu are based on 32-channel linear array multi-anodes. The tubes have been delivered without base. The photocathode material is bialkali and the window is made of borosilicate glass. The effective area per channel is $0.8 \times 7 \text{ mm}^2$ with a pitch of 1 mm. Our tubes have an average anode luminous sensitivity of $S_a = 374 \text{ A/lm}$ (according to data sheet 140 A/lm is typical), an average cathode luminous sensitivity $S_k = 84 \mu\text{A/lm}$ ($70 \mu\text{A/lm}$ typical), and an average gain $G = 4.4 \cdot 10^6$ ($2 \cdot 10^6$ typical). The gain uniformity between anodes lies between 1:1.1 and 1:1.25 (1:1.5 typical), with the edge anodes having slightly lower gains on average. Hardly any strip has less than 70% of the maximum gain in a given array. The photocathode sensitivity is defined as the ratio of the cathode current I_k (less the dark current) to the incident flux Φ , expressed in photometric units: $S_k(\text{A/lm}) = \frac{I_k(\text{A})}{\Phi(\text{lm})}$

Instead of supplying dynode voltages through a voltage divider, the phototubes are powered by individual Cockcroft-Walton bases, manufactured by

HVSys, Dubna. The dc voltage is pulsed and converted with a voltage doubler ladder network of capacitors and diodes to higher voltages. The principal advantage is that there is no need for stiff high voltage cables, since only ~ 140 V has to be distributed to the first front-end board, where the voltage is daisy-chained to the other boards of the detector plane. one drawback is that the voltages can only be equally spaced, which is acceptable for their actual use.

The first prototypes were designed for 128 fibres packed in 4 double layers in 0° column angle configuration, with a pitch of 0.6 mm between adjacent columns. Such a geometry implies an incident angle for scattered electrons of 0° . For a set-up in the electron focal plane of the KaoS spectrometer, this column angle is not appropriate since the scattered electrons have an inclination angle of $50 - 70^\circ$ with respect to the normal of the focal plane. Instead, a configuration with a column angle of $\alpha = 60^\circ$ and hexagonal packing has been chosen. The hexagonal packing, in which the centres of the fibres are arranged in a hexagonal lattice, and each fibre is surrounded by 6 other fibres, has the highest density of $\frac{\pi}{\sqrt{12}} \simeq 0.9069$. A prototype triple detector with this configuration is shown in Fig. 2. The small space between adjacent triple boards, with a pitch of only 79.6 mm, poses some difficulties on positioning and alignment. The small dimension of the dynode channels on the electrode plate, 0.8 mm, and the diameter of the fibres, 0.83 mm, makes it clear that the alignment has to be very precise.

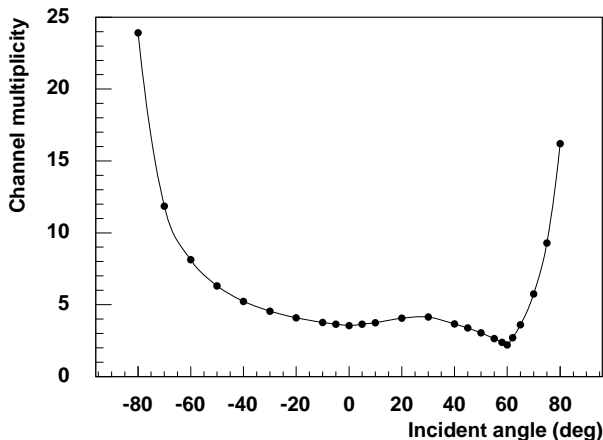


Figure 3: Simulated variation of the channel multiplicity as a function of the incident angle for a fibre array configuration with 60° column angle. The incident angles in the electron focal plane are distributed between $50^\circ - 70^\circ$.

Multiple scattering through small angles is given by the Gaussian width $\theta_0 = \theta_{plane}^{RMS} = 13.6 \text{ MeV} \frac{(z=1)}{(\beta=1)_{cp}} \cdot \sqrt{x/X_0} \cdot (1 + 0.038 \ln x/X_0)$ [3, 4]. The amount of scattering depends primarily on the momentum and the thickness of the scattering medium (radiation

length $X_0 = 42.4$ cm for a polystyrene scintillator). In the focal plane detector the latter depends also slightly on the momentum because tracks for different momenta pass the focal plane detector at different places under slightly different angles. The detector configuration leads to a thickness variation of $\pm 40\% \approx \pm 0.3$ mm/layer. The average thickness and its variation was simulated for electrons traversing the focal plane to be $x = (4.70 \pm 1.29)$ mm. This number translates into a width of $\theta_0 = 0.227^\circ$ for $p = 300 \text{ MeV}/c$. The main consequence of the incident angle distribution is an increased channel multiplicity. The pure geometrical effect was studied in a simulation of a 60° detector, the full calculation is shown in Fig. 3. The incident angles in the electron focal plane are distributed between $50^\circ - 70^\circ$.

1.2. Development of new Read-Out Electronics

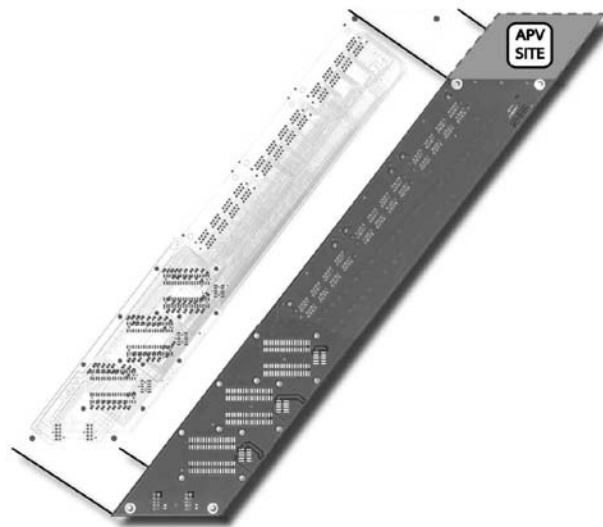


Figure 4: Photograph and circuit scheme of the triple front-end board showing the three PMT sockets at the lower left, and the output sockets. The site for the APV chip connector is indicated.

A 12-layer front-end board able to accommodate three 32-channel multi-anode photomultipliers with minimum time jitter was designed, see Fig. 4. It houses the low voltage power supply for the Cockcroft-Walton voltage multiplier bases, the RJ-45 connectors for analogue output to the discriminators and, in the near future, APV25 chips for amplifying, sampling and multiplexing the signal amplitudes.

Two 32-channel discriminator discriminator boards each housing 8 DTD chips have been prototyped by the electronics workshop of the Institut für Kernphysik, see Fig. 5 (left) for a photograph of the DTD board. The DTD boards have two multiplexed Lemo

analogue outputs for debugging and two LVDS outputs, one to be connected to TDC modules, and one to trigger modules. A 32-channel analogue output board can be attached to the discriminator board for a complete analysis during the prototyping stage. Up to 20 DTD boards fit into a VME 6U crate together with a controller board, see Fig. 5 (right) for a photograph. The communication with a PC is done via parallel port. The trigger will be derived with GSI VME logic modules. Such a module is equipped with a FPGA, and a large number of front panel inputs and outputs. The timing is picked off by TDC CATCH boards. These boards, developed for the COMPASS collaboration, are equipped with 4 mezzanine cards for a total of 32 channels. At the heart of the TDC mezzanine cards there are the so-called $\mathcal{F}1$ chips, developed by the Faculty of Physics of the University of Freiburg, Germany, with 8 channels of ~ 120 ps resolution (LSB) each.

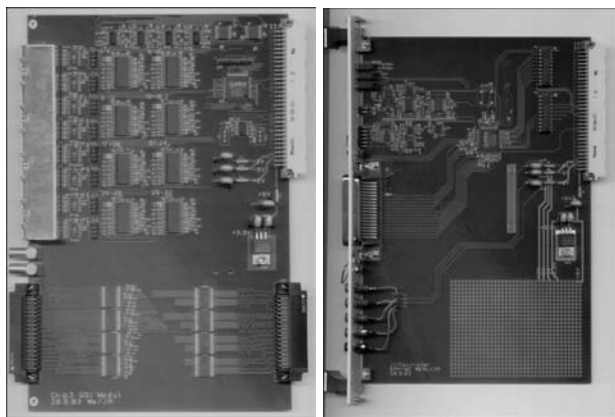


Figure 5: Left: photograph of the double threshold discriminator board. The two LVDS outputs are visible near the bottom of the module. The RJ-45 inputs are located at the top left of the module and the two Lemo outputs at centre left. Right: photograph of the controller board for up to 20 double threshold discriminator boards.

In addition to timing and trigger, an ADC system capable of handling high channel counts is also needed. For this purpose, another component of the COMPASS electronics is under investigation, namely the electronics around the APV-Chip and the GeSiCa data collector card. This system has been mainly developed by the Faculty of Physics of the Technical University of Munich, Germany, for the RICH sub-detector of the COMPASS set-up. With 128 input channels, each performing synchronous analogue sampling at 40 MHz, the APV chip acts as an analogue ring-buffer, which on demand multiplexes the appropriate 128-channel sample and sends it to an attached ADC. The GeSiCa module provides a similar functionality as the CATCH module, i.e. set-up of the attached front-end electronics, TCS information processing, data col-

lection, data concentration and data transfer to PC-based read-out buffer cards via SLink.

1.3. Prototype Fibre Detector Characterisation at the Electron Beam

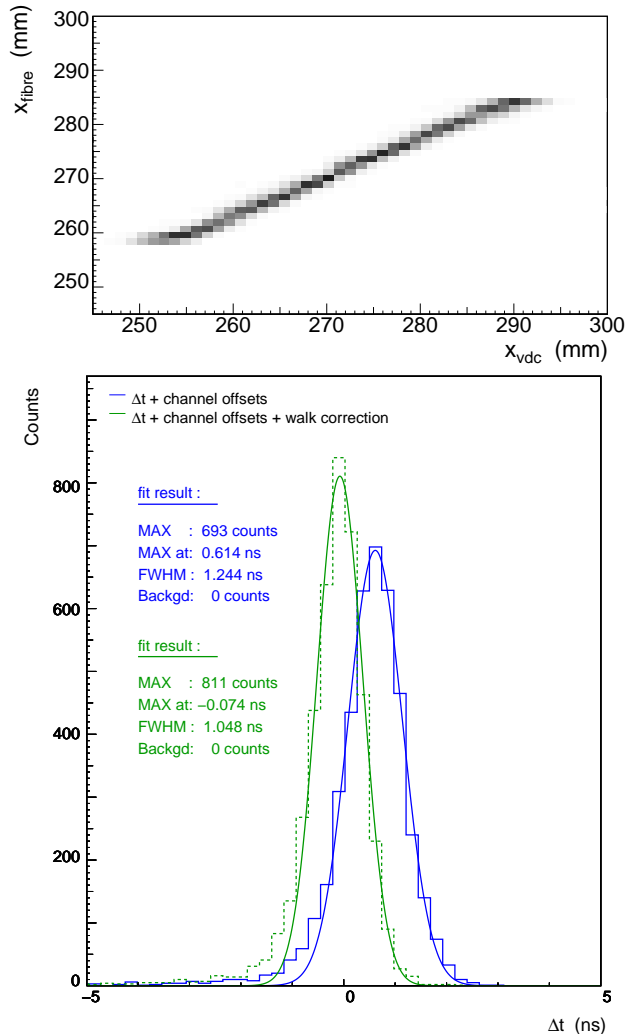


Figure 6: The top panel shows the reconstructed x -position of the electron projected onto the base coordinate versus the measured x -position obtained with a simple estimator from the fibre detector. The bottom panel shows the time resolution of the fibre detector obtained from the coincidence timing with the scintillator paddle detectors.

We have employed spectrometer A of the three spectrometer facility at MAMI to carry out a characterisation of a 32-channel fibre detector prototype. The detector was sandwiched between the drift chambers and the scintillator paddles of the focal plane detector system. The arrival time of the electrons was measured in the fibre detector with respect to the following two overlapping paddles. The electron

track was reconstructed with the position information of the drift chambers and the electron hit position was extrapolated from the drift chamber planes to the fibre detector plane. A simple estimator for the x -position $x = \sum_{i=1}^N x(\text{fibre}_i)/N + \text{offset}$ was used, where $x(\text{fibre}_i)$ is the geometrical position of the i th fibre and N the hit multiplicity. That position is compared to the reconstructed x -position of the electron projected onto the detector base coordinate, see Fig. 6 (top). Small non-linearities at the edges indicate that better estimators are needed. However, position estimators based on weighted averages suffer from fluctuations in pulse heights. Fig. 6 (bottom) shows the time resolution obtained from the coincidence timing with the scintillator paddle detectors after walk correction of the paddle timing. The FWHM of ≈ 1 ns is rather good for the small amount of light from the fibres.

2. Hypernuclear Gamma-Spectroscopy with PANDA at GSI

At $\bar{\text{PANDA}}$ relatively low momentum Ξ^- can be produced in $\bar{p}p \rightarrow \Xi^- \bar{\Xi}^+$ or $\bar{p}n \rightarrow \Xi^- \bar{\Xi}^0$ reactions [5]. The advantage as compared to the kaon induced reaction is the fact that the antiproton is stable and can be retained in a storage ring. This allows a rather high luminosity even with very thin primary targets. The associated $\bar{\Xi}$ will undergo scattering or (in most cases) annihilation inside the residual nucleus. Strangeness is conserved in the strong interaction and the annihilation products contain at least two anti-kaons that can be used as a tag for the reaction.

Because of the two-step process, spectroscopic studies, based on the analysis of two-body reactions like in single hypernuclei reactions [6], cannot be performed. Spectroscopic information on double hypernuclei can only be obtained via their sequential decay, see e.g. [7]. In combination with the high luminosity at FAIR and with a novel solid-state micro-tracker, high resolution γ -ray spectroscopy of double hypernuclei and Ω atoms will become possible for the first time.

It is intended to further develop existing HPGe detectors for γ -ray spectroscopy in order to use them in the presence of high particle fluxes and high magnetic fields. This will be achieved by new read-out schemes and tracking algorithms, which have to be developed. These studies will include the modelling of detector response and detailed background studies.

At present, it is foreseen to use a number of Euroball cluster detectors [8], partially owned by GSI, and in addition the use of the Vega detectors [9] of GSI.

Standard electronic readout systems are hardly capable of dealing with particle rates exceeding 10 kHz. However, the fully digital electronic system currently developed for the new generation of Ge arrays like

Vega will – in connection with fast preamplifiers – allow the load of background particles at rates higher than 100 kHz for each detector element. Arranging several cluster detectors and taking into account that most of the produced particles are emitted into the forward region not covered by the Ge array an interaction rate of 10^7 s^{-1} seems to be manageable.

The Euroball cluster consists of seven large hexagonal tapered Ge detectors closely packed in a common cryostat. The crystals have a length of 78 mm and a diameter of 70 mm at the cylindrical end. The super-segmented clover detector Vega has been developed at GSI. It consists of four coaxial four-fold segmented Ge detectors of 140 mm length and 70 mm diameter enabling an optimal arrangement with respect to efficiency and spectrometer response. Prior to the measurements the energy resolution of the detectors was deduced with a ^{60}Co source. The Vega detector as well as three of the seven crystals of the Euroball cluster detector were then set up inside the ALADiN magnet. A noisy environment was the cause of the non-perfect resolutions measured without a magnetic field.

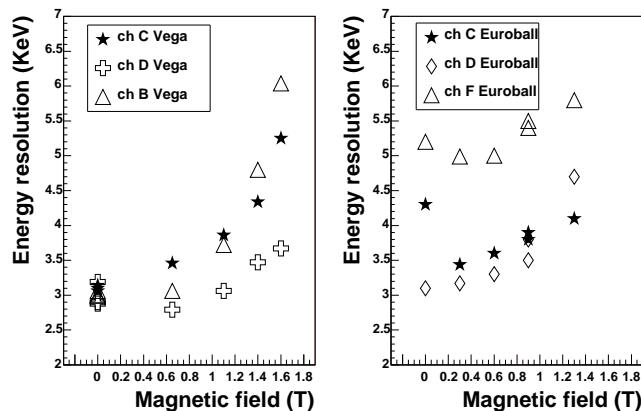


Figure 7: Measured energy resolution (FWHM) of Euroball cluster and Vega detectors in a magnetic field.

Fig. 7 shows the energy resolution (FWHM) at 1.33 MeV of three crystals of each detector as a function of the magnetic field. The energy resolution of one of the Euroball crystals was found to be worse than the others because of pick-up noise in its electronic readout, whereas two other crystals of the same detector showed a similar behaviour in the magnetic field. Their energy resolution slightly exceeded 0.3% at 1.2 T which, however, allows to perform γ -ray spectroscopy on hypernuclei. A similar behaviour was found for the Vega detector. For ADC spectra taken without magnetic field, a Gaussian distribution was chosen for fitting. In case the magnetic field was non-zero, a fit to a peak is composed of three components: a Gaussian, a skewed Gaussian, and a smoothed step function to increase the background on the low-energy side of the peak.

The ALADiN magnet aperture allows to set the detector only with its axis in the horizontal plane if the highest magnetic field should be present in the sensitive part of the detector. Then, the direction of the magnetic field lines is perpendicular to the detector axis. However, the energy resolution of the Vega detector was also measured for other angles. The results obtained indicated no deviation for 30° at a field of $B \sim 0.3$ T [12].

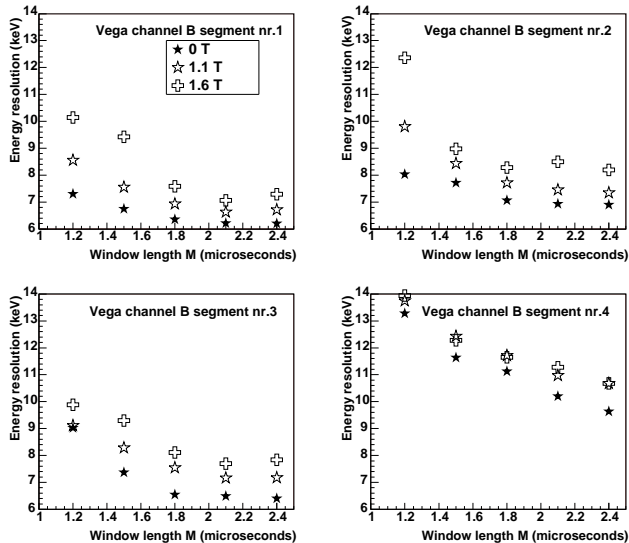


Figure 8: Measured energy resolution for 4 segments of Vega channel B as a function of the deconvolution window width for different values of the magnetic field.

The measurements were performed over a period of two days without observing any problems with FETs, vacuum breaks or sparking of the crystals. After the measurements the original energy resolution was recovered.

For the measurements of the pulse shape, a SIS3300 8-channel 100 MHz 12-bit FADC was used. It was directly connected to the preamplifier of one of the channels of Vega. The scope of this analysis was the extraction of the energy resolution from the preamplifier signal by using digital signal processing. The output signal of a charge integrating preamplifier with continuous discharge consist of a fast rising step due to the charge collection, followed by an exponential tail due to the discharge of the capacitors over the resistor. The exponential tail reduces the final peak height depending on the rise time of the signal, therefore in order to extract the whole amplitude of the signal which corresponds to the energy of a gamma ray, the influence of the preamplifier has to be removed. This is accomplished by the moving window deconvolution algorithm (MWD) [11].

It consists of two parts: the first part is a deconvolution, which transforms the continuous discharge preamplifier signal into a staircase signal. By applying numerical differentiation of such a signal the moving window deconvolution equation is obtained. It con-

verts an exponential signal into a step signal of length M , M being the width of the deconvolution window. Knowing the decay time and the start time of the signal, the initial amplitude can be determined from any data point of the decaying signal. The decay time for Vega detectors is about $50 \mu\text{s}$.

In Fig. 8, the energy resolution of the 4 segments of the analysed channel at Vega, extracted by using the method explained above, is shown as a function of the deconvolution window length M for different values of the magnetic field. Even though each segment shows a different character, all segments exhibit a common trend, i.e. the energy resolution improves with longer FADC sampling times. The pulse shape is evidently affected at high magnetic field. With these measurements the investigation of the feasibility of Ge detectors under high magnetic fields was fully addressed [12].

Acknowledgments

We acknowledge financial support from the Bundesministerium für Bildung und Forschung (bmb+f) under contract number 06MZ176. This research is part of the EU integrated infrastructure initiative HadronPhysics Project under contract number RII3-CT-2004-506078.

References

- [1] P. Senger et al. (KaoS Collaboration), Nucl. Inst. & Meth. in Phys. Res. **A327**, 393 (1993).
- [2] P. Achenbach et al. (A1 Collaboration), experiment proposal MAMI-A1/1-03, Mainz Microtron MAMI (2003).
- [3] H. Bethe, Phys. Rev. **89**, 1256 (1953).
- [4] W. Scott, Rev. Mod. Phys. **35**, 231 (1963).
- [5] PANDA Collaboration, *Technical progress report for PANDA: strong interaction studies with antiprotons* (GSI, Darmstadt, 2005).
- [6] M. Agnello et al., Phys. Lett. B **622**, 35 (2005).
- [7] S. Aoki et al., Prog. Theor. Phys. **85**, 1287 (1991).
- [8] J. Eberth et al., Nucl. Inst. & Meth. in Phys. Res. **A369**, 135 (1996).
- [9] J. Gerl et al., in *Proc. of the Conf. on Physics from Large γ -ray Detector Arrays, Berkeley, USA* (1994), p. 159.
- [10] A. Sanchez Lorente et al., in *GSI Sci. Rep. 2004* (GSI, Darmstadt, 2005), FAIR-EXP-23, p. 32.
- [11] A. Georgiev, W. Gast, and R. Lieder, IEEE Trans. Nucl. Sci. **41**, 1116 (1994).
- [12] A. Sanchez Lorente et al., in *GSI Sci. Rep. 2005* (GSI, Darmstadt, 2006).